Meso-Cenozoic deformation history of Thailand; insights from calcite U-Pb geochronology

Alexander Simpson[1], Stijn Glorie[1], Chris K Morley[2], Nick M W Roberts[3], Jack Gillespie[1], Jack K Lee[3,4]

[1]Department of Earth Sciences, The University of Adelaide, SA 5005, Australia

[2]Chiang Mai University, 239 Huaykaew Road, Tumbol Suthep Amphur Muang, Chiang Mai, Thailand

[3]Geochronology and Tracers Facility, British Geological Survey, Keyworth NG12 5GG, UK

[4]Department of Earth Sciences, University of Durham, Science Labs, Durham

Corresponding author: Alexander Simpson (a1193000@adelaide.edu.au)

Key Points:

- Novel *In-situ* LAICPMS U-Pb calcite dates constraining tectonic activity in Thailand
- Calcite chemistry used to distinguish different growth event associated with fault movement

Abstract

Given the general absence of suitable direct dating methods, the timing of low-temperature crustal deformation is usually established by indirect methods (such as apatite fission track (AFT) thermochronology), and through relative field-based relationships. U-Pb dating of calcite in tectonic veins represents a recently developed method to directly date brittle deformation. Here, we apply this method to tectonic calcite veins in large scale fault zones in central and western Thailand, in an attempt to shed new light on the regional upper crustal deformation history. U-Pb calcite dates demonstrate tectonic activity at ~216-209 Ma in the Khao Kwang Fold and Thrust Belt associated with the Indosinian stage 2 collision between the Sibumasu and the Indochina Blocks. Brittle deformation along the Three Pagodas Fault Zone has a protracted history, with calcite dates from a single locality at ~45 Ma and ~23 Ma. Petrographic techniques such as reflected light and charge contrast imaging, combined with LA-ICP-MS elemental mapping, are used to relate the U-Pb dates with the paragenesis of the calcite veins in relation to phases of brittle faulting and associated fluid-flow. The veins are interpreted to have formed during multiple hydraulic fracturing events along single fault planes, and exhibit contrasting trace elemental signatures implying fluids with contrasting chemistries have infiltrated the vein arrays during different brittle deformation events. The results from this study advance knowledge on the multi-phase deformation history of Thailand and illustrate the application of combined U-Pb dating and trace element mapping in calcite to unravel complex upper crustal tectonic histories.

1 Introduction

A variety of techniques have been used to constrain the geological history of Thailand, from U-Pb and Ar-Ar dating of igneous and metamorphic minerals to biostratigraphy of syn-kinematic sequences and unconformable relationships [*Hansen and Wemmer*, 2011; *Lacassin et al.*, 1997; *C K. Morley and Andrew Racey*, 2011; *Morley et al.*, 2011; *Ridd et al.*, 2011; *Ueno and Charoentitirat*, 2011; *Ueno et al.*, 2010]. However, the exact timing of major tectonic events that affected Thailand, such as the onset and extent of the Indosinian Orogeny, remain controversial [e.g. *Morley et al.*, 2013]. Similarly, the timing of Cenozoic deformation, in relation lateral extrusion in response to the India-Eurasia collision [*Rhodes et al.*, 2005] is established from biostratigraphic dating of sedimentary basins [as reviewed by *C K. Morley and Andrew Racey*, 2011]), from radiometric dating of ductile deformation in a limited number of localities [e.g. *Gardiner et al.*, 2016; *Lacassin et al.*, 1997; *Watkinson et al.*, 2011]and from radiometric cooling ages inferred to be related to uplift and erosion in response of fault motion [*Morley*, 2009; *Nachtergaele et al.*, 2019; *Upton*, 1999]. However, dating of individual structures in sedimentary sequences is typically highly imprecise and often it is difficult to justify whether a particular fault or fold in a Palaeozoic unit is related to Triassic or Cenozoic events, or even some more poorly defined event of a different age. Our inferences about the timing of such structures in Palaeozoic carbonates provides an excellent framework to both explore U-Pb dating of tectonic calcite veins and to increase our understanding of Thailand's geological history.

Two locations were chosen for this study, the Khao Kwang Fold and Thrust Belt (KKFTB) and the Three Pagodas Fault Zone (TPFZ), which both record complex tectonic histories. Previous studies indicate that these locations were active during major tectonic events during Thailand's geological history, such as the Triassic Indosinian Orogeny, and Palaeogene strike-slip escape tectonics [*Morley et al.*, 2011; *Morley et al.*, 2013], but both lack robust constraints on the timing of brittle faulting and fracturing events that affected Ordovician and Permian carbonate sequences.

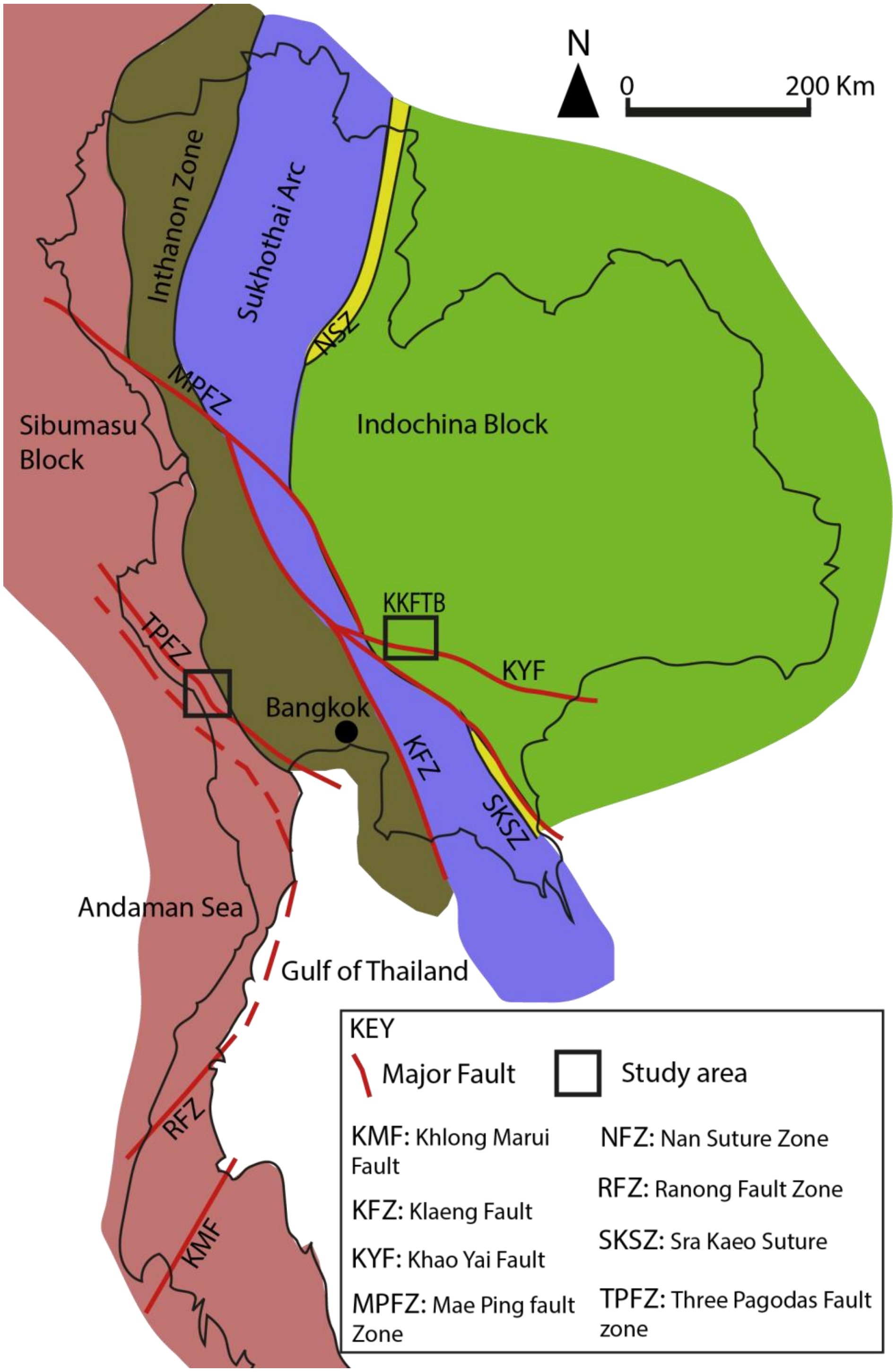

Figure 1. Simplified geological map of Thailand. A shows the KKFTB sampling area. B shows the TPFZ sampling area. (Based on Sone & Metcalf, 2008 and Warren et al, 2014).

The Khao Kwang Fold and Thrust belt (KKFTB, Fig. 2) formed during the Indosinian Orogeny [*Morley et al.*, 2013]. Zircon U-Pb dates on granitoid intrusions [*Dew et al.*, 2018b; *Morley et al.*, 2013] and U-Pb dating by detrital zircons, which established maximum depositional ages of Triassic units deposited during the Indosinian orogeny [*Arboit et al.*, 2016], have provided high temperature insights into the tectonic history of the area. Low-temperature constraints are limited. Few K-Ar dates on authigenic illites within thrust fault zones [*Hansberry et al.*, 2017] have yielded Triassic ages, in addition to a few ~39 – 19 Ma apatite fission track dates, which indicate the timing of exhumation, possibly related in part to strike-slip fault activity [*Upton*, 1999].

The Three Pagodas Fault Zone (TPFZ) in western Thailand (Fig. 1) represents a Cenozoic structure that developed in response to the India-Eurasia collision [e.g. Lacassin et al., 1997; Morley, 2002; *Rhodes et al.*, 2005]. ^{40}Ar-^{39}Ar dates, obtained from micas in gneisses within the TPFZ, suggest that ductile (left-lateral) slip occurred during the late Eocene – early Oligocene [*Lacassin et al.*, 1997], which broadly agrees with the timing of cooling and exhumation in the hinterland, defined by apatite fission track thermochronology [*Upton*, 1999]. Direct constraints on the timing of brittle faulting in the TPFZ are, however, currently lacking. The TPFZ records complex structures such as unusual boudinaged, highly veined, layers in Ordovician carbonates [*Nazrul*, 2015], however, it has yet to be demonstrated whether these structures are of Cenozoic age, or related to older events such as the Indosinian Orogeny or represent multiple fault reactivation events.

Hence, both of the selected study areas contain extensive calcite veining that can be linked to major structures that deformed the study areas [e.g. *Hansberry et al.*, 2014; *Hansberry et al.*, 2015] but lack absolute time constraints on brittle faulting. Previous studies [*Li et al.*, 2014; *Nuriel et al.*, 2017; *Roberts and Walker*, 2016] have demonstrated that *in-situ* laser ablation inductively coupled mass spectrometry (LA-ICP-MS) U-Pb dating of calcite veins can produce direct constraints on the timing of calcite growth. While crack-seal calcite veins [see *Bons et al.*, 2012] are preferable for dating due to their textural link to fault movement [*Bons et al.*, 2012; *Roberts and Walker*, 2016], there are a range of possibly syn-tectonic calcite textures that are worth exploring with this novel technique. Using field-relations and petrography to link calcite mineralisation to brittle deformation, calcite U-Pb geochronology has the potential to directly date brittle deformation in the KKFTB and TPFZ. Here we present calcite U-Pb results to unravel the timing of brittle faulting along both the KKFTB and TPFZ in Thailand, and we discuss how coupled U-Pb dating with trace element mapping can be used to differentiate different fluid generations that can be related to fault (re)-activation in the study areas.

2 Geological setting and field site descriptions

2.1 Regional Tectonic History

Thailand can be geologically subdivided into the Sibumasu Block (in the west) and the Indochina Block (in the east) [see *Morley*, 2018; *Ridd et al.*, 2011; *Sone and Metcalfe*, 2008] (Fig. 1). These terranes are separated by the remnants of an overthrust accretionary complex (The Inthanon Zone) and a Palaeozoic island arc (Sukhothai Arc) [*Ridd et al.*, 2011] (Fig. 1).

Given the similarity of its upper Palaeozoic stratigraphy with other Gondwana-derived terranes, the Sibumasu Block likely represents a fragment of the northern margin of Gondwana, [*Ueno et al.*, 2010]. The Sibumasu Block likely rifted off Gondwana during the early Permian, before colliding with Indochina (as part of Eurasia) during the Paleo-Tethys closure [*Barber et al.*, 2011; *Dew et al.*, 2018b]. The Sukhotai Arc rifted from the Indochina Block at a roughly similar time [*Barr and Macdonald*, 1987]. The timing of tectonic events associated with the Indosinian Orogeny are highly controversial [*Morley*, 2018], in part because there has been very little radiometric dating of Indosinian structures. Instead, the timing of events is based on unconformities (that are often poorly dated), or the timing of orogeny-related sedimentary units, metamorphic and igneous events (Morley, 2018). The so-called Indosinian 1 and 2 events (Booth and Sattayarak, 2011), are probably only local events confined to the Khorat Plateau area, and may not represent orogen-wide events [*Morley*, 2018]. The problems of understanding the timing of events emphasises the need for new techniques to better date the structural history associated with the Indosinian orogeny in SE Asia.

2.2 Khao Kwang Fold and thrust Belt

The Khao Kwang Fold and Thrust Belt (KKFTB) is situated on the western edge of the Indochina Block in the Saraburi Province (Fig. 2). The KKFTB is composed of deformed mixed siliclastic-carbonate sediments that were deposited during the Permian to early Triassic [*Dew et al.*, 2018a]. This location is characterised by WNW-ESE to NE-SW oriented thrusts and folds [*Morley et al.*, 2013]. Recent work suggests that extensive sedimentation occurred between ~250 Ma and 205 Ma within piggyback basins that developed on top of thrust-sheets in the foreland of the Indosinian Orogen [*Arboit et al.*, 2016]. The timing of sedimentation in such syn-tectonic basins, combined with authigenic illite dates within the KKFTB [*Hansberry et al.*, 2017], imply a major period of deformation that began around 250 – 240 Ma and lasted until ~225 Ma (Indosinian Stage 1). However, structural observations [*Arboit et al.*, 2015; *Morley et al.*, 2013] suggest that subsequent deformation events have occurred in the region in differing paleo-stress regimes, as demonstrated by an authigenic illite date from a fault zone of ~208 Ma [*Hansberry et al.*, 2017], as well as more recent (~205 Ma) detrital zircon dates [*Arboit et al.*, 2016] from folded and cleaved clastics. Hence, Indosinian deformation recorded in the KKFTB was likely long-lived, lasting until at least ~205 Ma

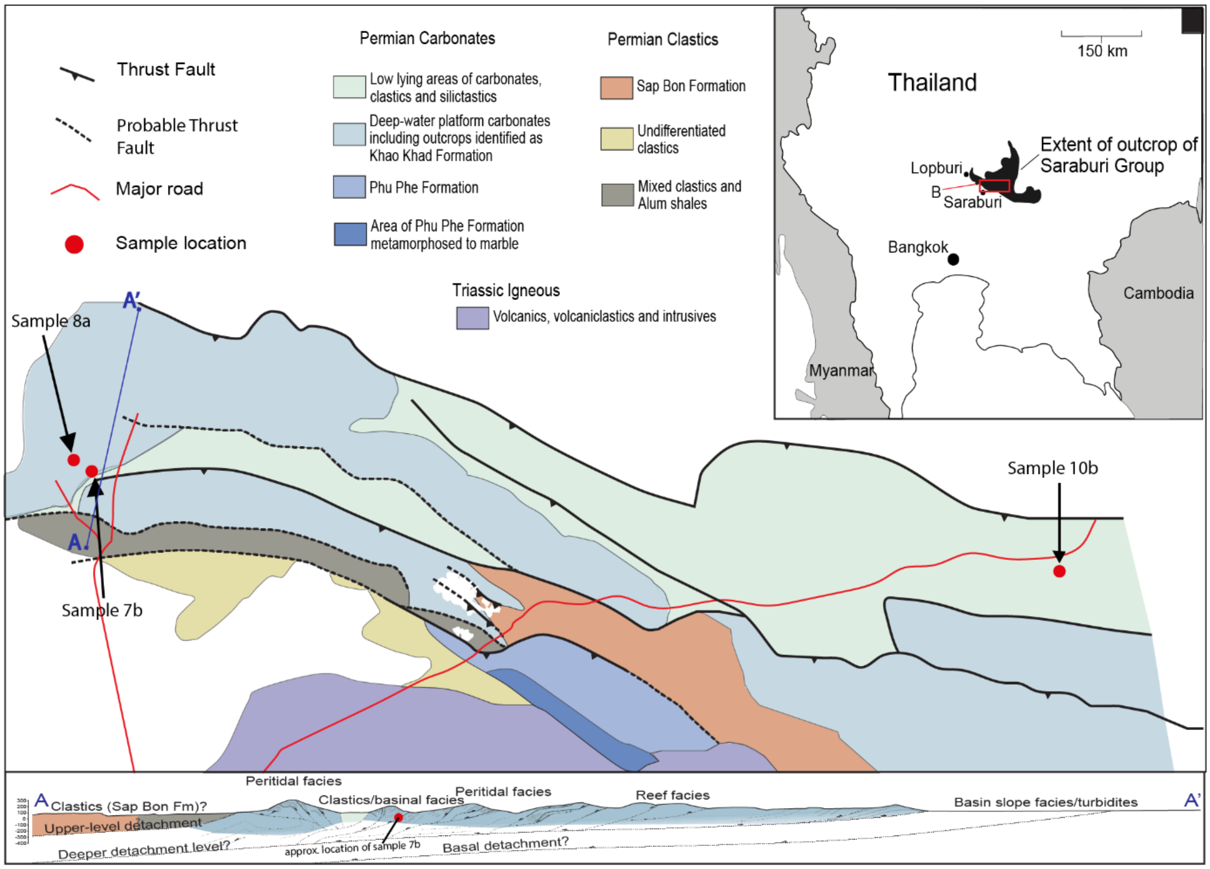

Figure 2. Simplified geological map of the KKFTB showing sample locations. Based on Morley et al, 2013; Hansberry et al, 2015)

Calcite veining, linked to fluid flow during orogenesis has previously been identified in the KKFTB [*Arboit et al.*, 2017; *Hansberry et al.*, 2015; *Warren et al.*, 2014]. Since matrix permeability decreased during orogenesis, fluid was concentrated along shear zones and fractures [*Warren et al.*, 2014]. Calcite was precipitated along these fractures potentially leading to a competency contrast between wall rock and precipitated calcite [*Hansberry et al.*, 2015]. This is interpreted to have led to a positive feedback loop, in which further faulting was concentrated along the plane of weakness created by the precipitated calcite [*Hansberry et al.*, 2015]. Thus, the calcite veining associated with faults and shear zones is predominantly syn-tectonic, and for large fault zones, likely multi-phase.

A complex post-Permian paleostress history for the KKFTB has also been determined from analysis of strained calcite in veins [*Arboit et al.*, 2015]. Analysis of stable O and C isotopes indicated that the temperature and origin of fluids filling the calcite veins have a complex and varied history including; early diagenetic cements, veins developed during burial, veins develop during various stages of the Indosinian orogeny, veins sweated out during episodes of igneous intrusions, veins formed during Cenozoic strike-slip activity, and late-stage veins related to uplift and karstification [*Warren et al.*, 2014]. In this study *in-situ* calcite U-Pb dating, coupled with trace element concentration imaging was applied to shed more light on the timing of this complex deformation history.

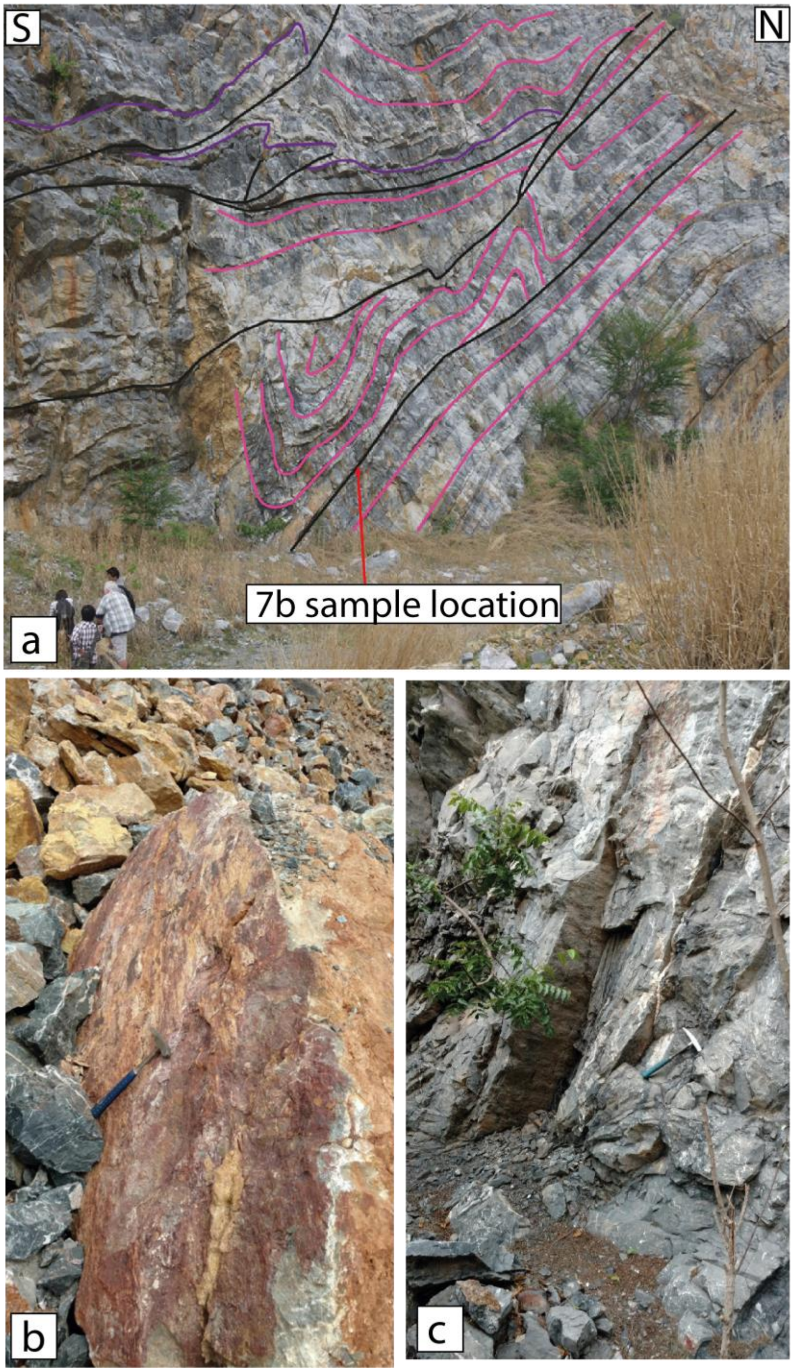

Figure 3. KKFTB sample location photos. A: sample 7b. B: sample 8b, and C: sample 10b

2.3 Three Pagodas Fault Zone

Situated within Kanchanaburi Province, the Three Pagodas Fault Zone (TPFZ) is characterised by a series of NW-SE trending strike-slip faults [*Morley*, 2002; *Rhodes et al.*, 2005] (Fig.1) and is estimated to be more than 700 km in length [*Searle and Morley*, 2011]. Two episodes of exhumation in the area are suggested by regional apatite fission track (AFT) studies at ~39 – 32Ma and ~24 – 19Ma [*Upton*, 1999], and both are thought to be related to the India-Eurasia collision and convergence [*Rhodes et al.*, 2005]. The first exhumation period coincides with mica Rb-Sr and Ar-Ar dates (~36 - 33 Ma) that are interpreted as being related to the late or final stages of Eocene – early Oligocene ductile left-lateral slip along the TPFZ [*Lacassin et al.*, 1997; *Nantasin et al.*, 2012].

Dating of syn-kinematic minerals [e.g. *Lacassin et al.*, 1997; *Palin et al.*, 2013] and structural observations (uplift associated with restraining bends) have been used to infer initial left-lateral transpressional activity (~39 – 32 Ma) along the TPFZ as well as the parallel Mae Ping Fault Zone [Fig. 1; *Morley et al.*, 2007]. U-Pb dating of zircon and monazite hosted in a metamorphic core complex exposed in the Mae Ping Fault zone suggest an earlier prograde metamorphic event at ~45 Ma [*Österle et al.*, 2019]. Additionally, tectonic activity at ~48 Ma has been identified on the nearby Ranong and Khlong Marui Faults [*Watkinson et al.*, 2011], suggesting this was a regional deformation event. Sinistral movement along the TPFZ was followed by a change to dextral transtensional activity (~24 Ma to present), as indicated by the development of pull-apart basins at releasing bend configurations [*Morley*, 2002; *Christopher K. Morley and Andrew Racey*, 2011; *Morley et al.*, 2011; *Rhodes et al.*, 2005]. The continued movement of India into Eurasia and resultant changes to the regional stress field have been posited as an explanation for the change from sinistral to dextral deformation [*Huchon et al.*, 1994; *Leloup et al.*, 2001; *Rhodes et al.*, 2005].

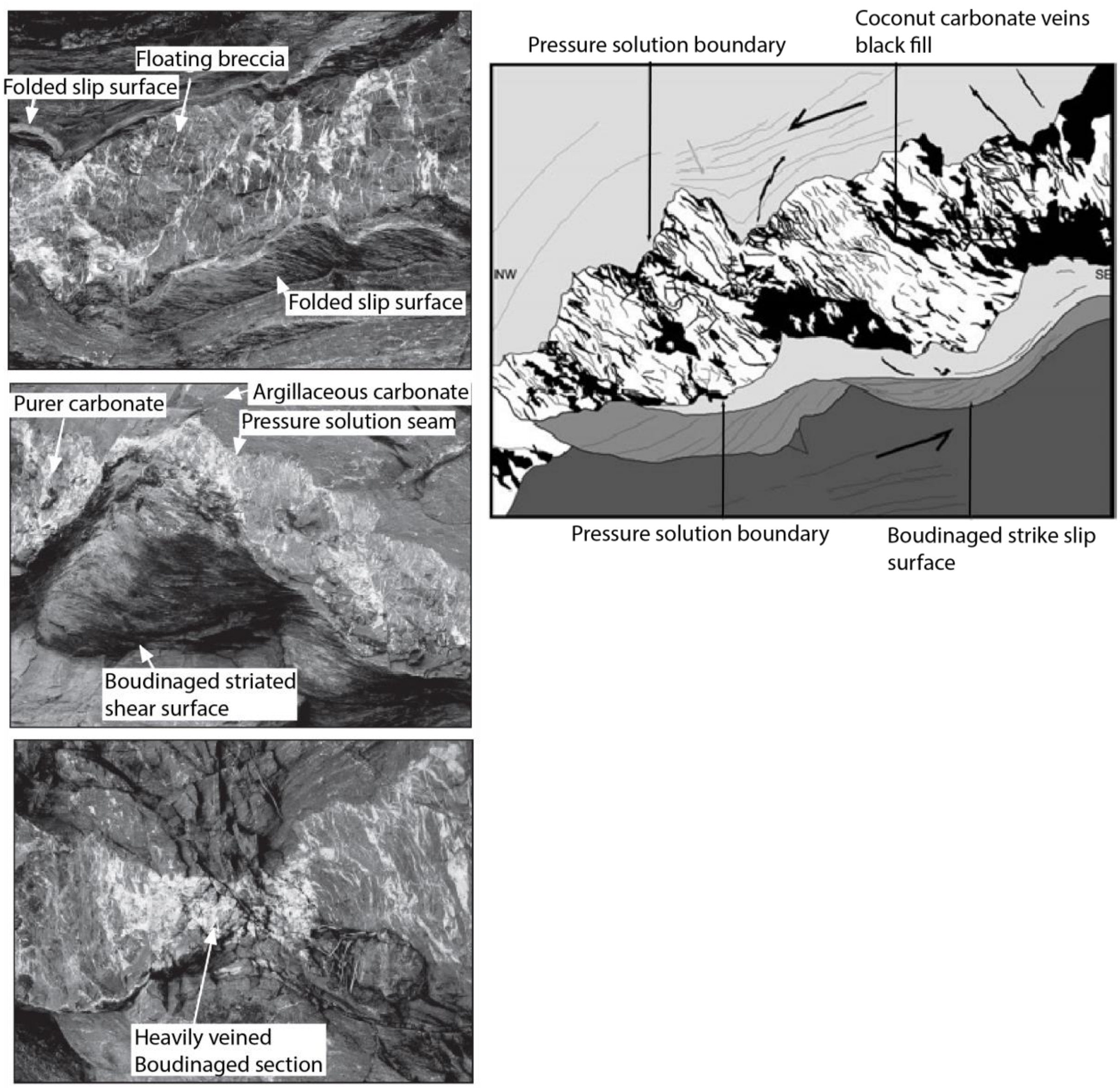

Figure 4. Interpreted photos and diagram of a floating clast breccia from the TPFZ (12a was sample location). Dark colour represents calcite veins in cartoon image.

The TPFZ is of particular interest due to the complex nature of the tectonic veins and other geological structures. Exposed splays of the TPFZ contain unusual vein filled boudinage-like structures (Fig. 4) that are interpreted to have formed due to strike-slip related pressure dissolution processes. These 'boudins' are tens of meters in length and 30 – 40 cm wide. As summarized by *Davies and Smith* [2006], fluid flow within a fault zone is episodic and related to stress build up to shear failure of the fault. Brine flow and resultant veining controlled by faulting will also be episodic [*Eichhubl and Boles*, 2000a; b]. Where the host rock has low permeability, the pressure transient caused by deformation cannot easily be lost by fluid flow. Instead, hydrofracturing occurs and the host rock is shattered to form a dilational breccia [floating clast breccia; *Sibson*, 1996]. The 'coconut texture' are commonly seen in hydrofractured carbonates, and tend to be associated with periods of thermochemical sulfate reduction (TSR), especially if there is some sulphate and organic material in the system [e.g. *Al-*

Aasm, 2003]. Hence, it is inferred that the veins evolved during an overpressuring event, were CO_2 rich, and were the result of periodic hydrofracturing. The floating clast breccia zones (Fig. 4) probably remained as sites of brine concentration. Following the abrupt generation of the breccia, pressure solution seams appear to have become preferentially located at the margins of the breccia where shortening was being accommodated

3 Materials and Methods

Calcite veins associated with the aforementioned structures were selected, targeting both crack-seal and hydraulic fracturing related calcite veins. Crack-seal veins are associated with repeated fracture and fill events that seal rapidly [*Bons et al.*, 2012]; thus, they should not display long lived open system behaviour, and calcite should precipitate broadly at the time of fracturing [*Roberts and Walker*, 2016]. The other type of samples are from dilational breccias, described above. Sample details are presented in Table 1. Of the nineteen samples that were screened for this work, only four samples provided robust U-Pb dates; these are the only samples considered further. Unsuccessful samples fall into the following two categories: (1) samples dominated by high common Pb; and (2) high analytical uncertainties that render an accurate regression impossible.

Selected calcite fragments from each sample were mounted in 1 inch epoxy mounts (for some samples multiple fragments were analysed). Sample imaging was conducted at the British Geological Survey, Nottingham, UK. Cathodoluminescence (CL) imaging was conducted with a Technosyn 8200 MKII cold-cathode luminoscope stage attached to a Nikon optical microscope with a long working distance lens, and equipped with a Zeiss AxioCam MRc5 digital camera. Vacuum and electron beam voltage and current were adjusted as required to generate optimum luminescence. Back-scattered electron and charge-contrast imaging were conducted using a FEI QUANTA 600 environmental scanning electron microscope (ESEM) with a working distance of 10 mm. BSE images were recorded using a solid-state (dual-diode) electron detector, with a 20 kV electron beam accelerating voltage, and beam currents between 0.1 and 0.6 nA,. Charge Contrast Images (CCI) were recorded using a FEI large-field gaseous secondary electron (electron cascade) detector, with 20 kV electron beam accelerating voltage, and beam currents of 1.2 to 4.5 nA.

LA-ICP-MS mapping was conducted at The University of Adelaide using an ASI resolution LR Laser Ablation System coupled to an Agilent 7900 mass spectrometer in order to identify zones with suitable U and Pb concentrations for dating purposes, as well as to identify growth zoning or alteration. Spot analysis was conducted using large spot sizes (110 microns) in order to maximise the signals from elements that were expected to have low concentrations. Only isotopes necessary for U-Pb dating (^{43}Ca, ^{202}Hg ^{204}Pb, ^{206}Pb, ^{207}Pb, ^{208}Pb, ^{232}Th and ^{238}U) were measured during spot analysis in order to maximise the dwell time on masses expected to have low abundance, such as the isotopes of Pb. Standard-sample bracketing was used, with the NIST614 glass reference material used for fractionation correction of the Pb-Pb ratios, and the WC-1 calcite reference material for correction of the U-Pb ratios [*Li et al.*, 2014; *Roberts and Walker*, 2016; *Roberts et al.*, 2017]. An in house calcite sample labelled 'Prague' of known stratigraphic age was used as an accuracy check [*Farkaš et al.*, 2016]. Instrumental settings for all runs are included in supplementary file X and the Concordia plots for the secondary standards are presented in supplementary figure 2 Data reduction was conducted using Iolite software

[*Paton et al.*, 2011]. Elemental map data was produced using the Monocle plugin for Iolite [*Petrus et al.*, 2017]. In more detail, polygons, termed regions of interest [*Petrus et al.*, 2017] surrounding the ablation spots were used to query elemental concentrations. Some spot analyses were removed based on anomalous chemistry related to alteration or different mineral fazes (e.g. clays), particularly high Al and U. Resulting calcite dates were calculated using isochron regressions in IsoplotR [*Vermeesch*, 2018] and are presented in Tera-Wasserburg concordia plots.

4 Results

4.1 Petrogpraphy

4.1.1 KKFTB samples

Sample 7b is a thin (1 – 2 mm) vein cross-cutting the limestone host rock, exhibiting blocky calcite growth that is common in calcite veins formed through hydrofracturing processes Fig. 5). The CL emission of this sample is dark, but with the exposure turned up, the sample reveals faint intra-crystal zonation (supplementary Fig. X).

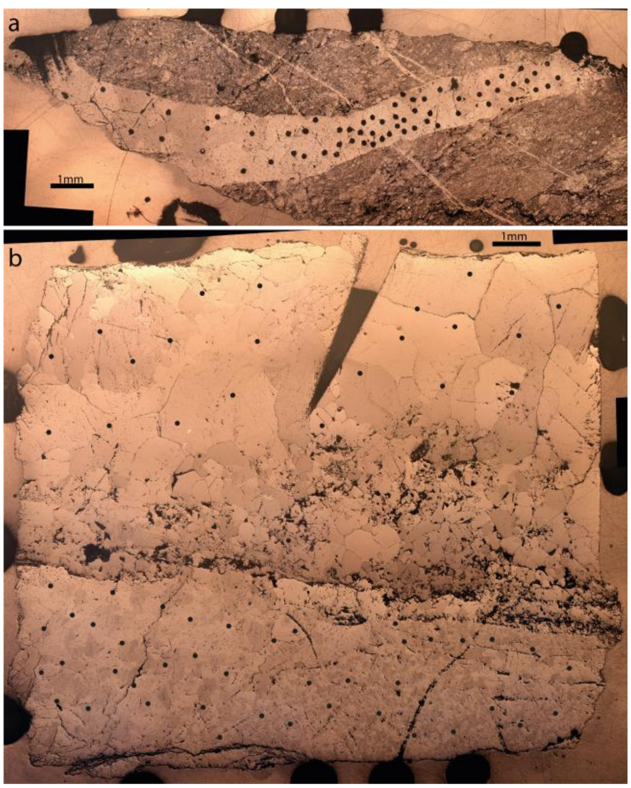

Figure 5. Reflected light images of samples 7b and 10b. Black circles represents ablation spots

Sample 8b (Fig. 6) is a several mm thick vein, exhibiting a clear primary cleavage that appears to be cross-cut by later generations of fluid-flow. These later veinlets are enriched in many trace elements such as Al and Mn (Fig. 6). The CL texture of the vein is fairly weak and homogeneous, except for the younger veinlets which are darker. CCI shows a planar fabric that is pervasive throughout the primary calcite at a shallow angle to the cleavage (Fig. 6). Such pattern is speculatively interpreted as low-temperature deformation twinning of Type 1 due to the narrow width of the twins and lack of recrystallization [*Ferrill et al.*, 2004].

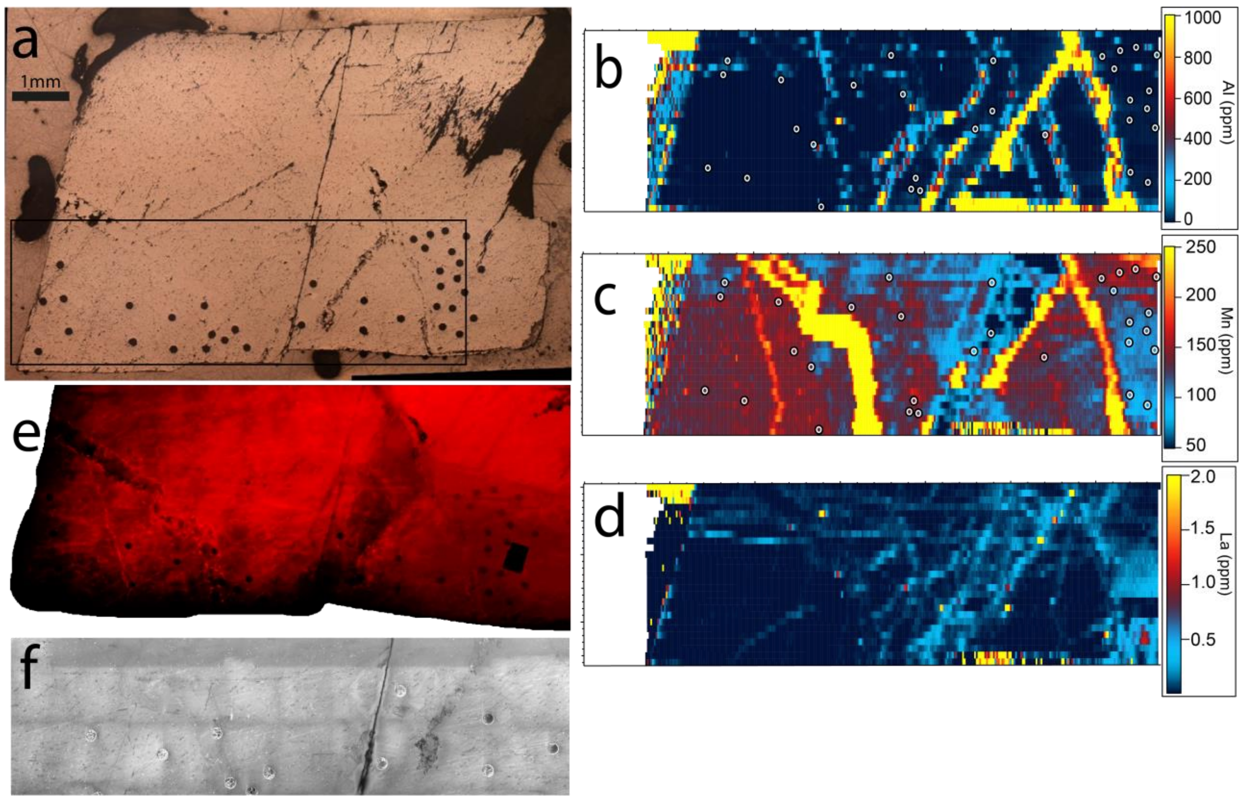

Figure 6. KKFTB sample 8b. **a:** High resolution reflected light image of sample 8b. Black rectangle shows elemental map area. **b:** Al elemental map. **c:** Mn elemental map. **d:** La elemental map. **e:** Cathodoluminescence (CL) image of sample 8b (brightness and contrast have been changed to highlight zonation. For elemental maps White and black circles show laser spot locations. **f**: CCI image of sample 8b interpreted to show type I low temperature twins

4.1.2 TPFZ sample

Sample 12a is a veinlet hosted within a limestone matrix. The crystal/grain boundaries are ragged, and may reflect overprinting during successive fluid-flow and/or a deformation event. The calcite has a very low CL response, and therefore, calcite crystal outlines and primary growth zoning cannot be ascertained (Fig. 7). In CCI, the calcite exhibits a planar fabric that is patchy in nature (Fig. 7). We interpret this to reflect high-temperature twinning [Type IV; *Ferrill et al.*, 2004], and dynamic recrystallization. The elemental zonation loosely correlates with the crystal boundaries visible in reflected light.

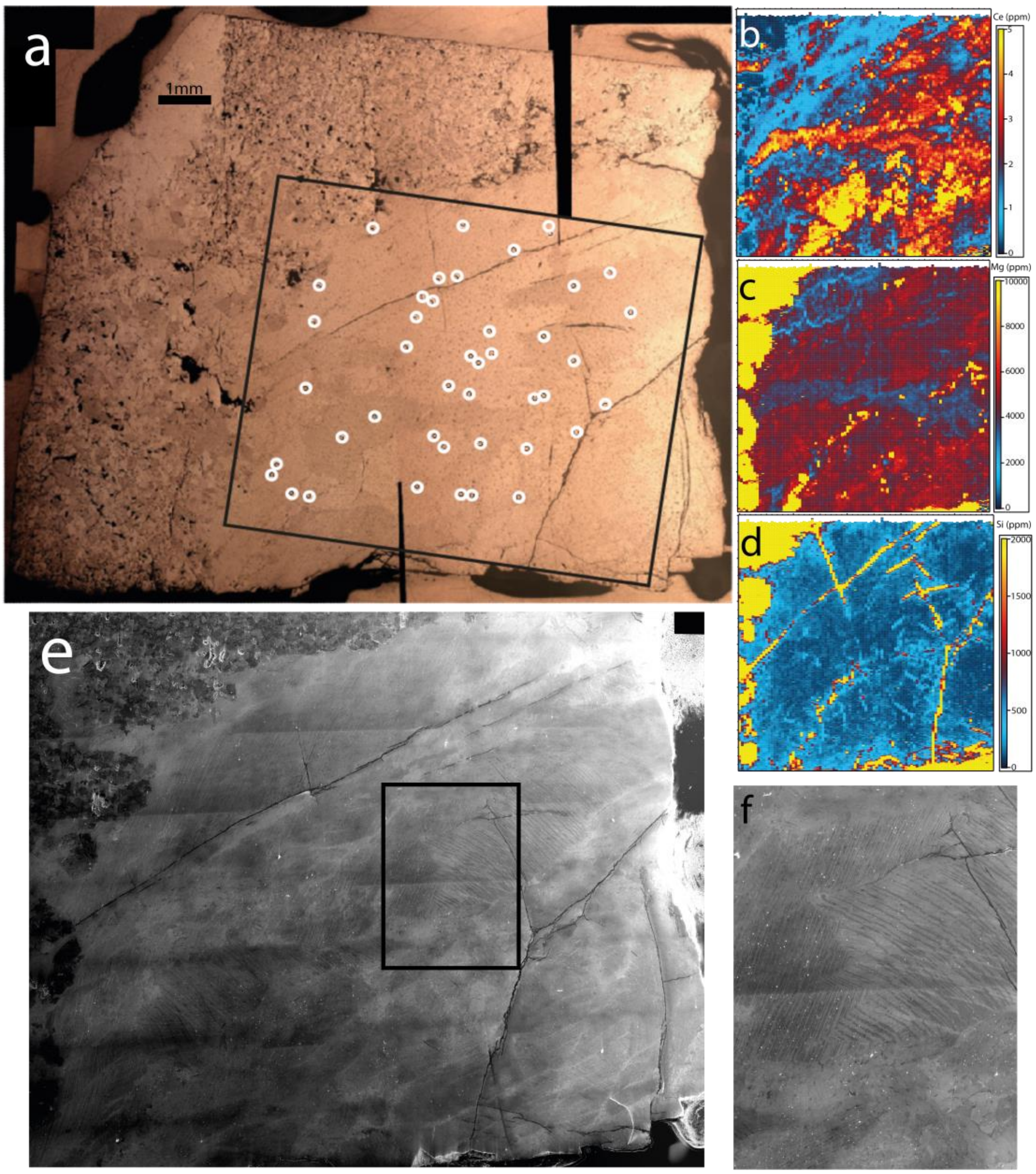

Figure 7: TPFZ sample 12a. **A:** Reflected light image of sample 12a. Black rectangle shows mapped area. White and black circles show laser spot locations. **B:** Si elemental map of sample 12a. **C:** Ce elemental map. **D:** Mg elemental map. **E**: CCI image of sample 12a. Black rectangle shows location of F. **F**: close up of CCI image demonstrating type 4 high temperature twins

4.2 U-Pb dating and Trace element geochemistry

For the four successful samples in this study, average U concentrations ranged from 0.292 – 1.86 ppm, and average total Pb concentrations ranged from 0.009 ppm – 0.226 ppm. Mean squared weighted deviation (MSWD) varied, with most being higher than 2.5. These high MSWD values, reflecting significant scatter in the data, suggesting that the absolute age and uncertainties should be treated with some caution. This may be due to heterogeneous common Pb, and mixed age components (see discussion section for details). The analytical precision ranged from <1% (sample 10b) to ~14% (sample 8b population A).

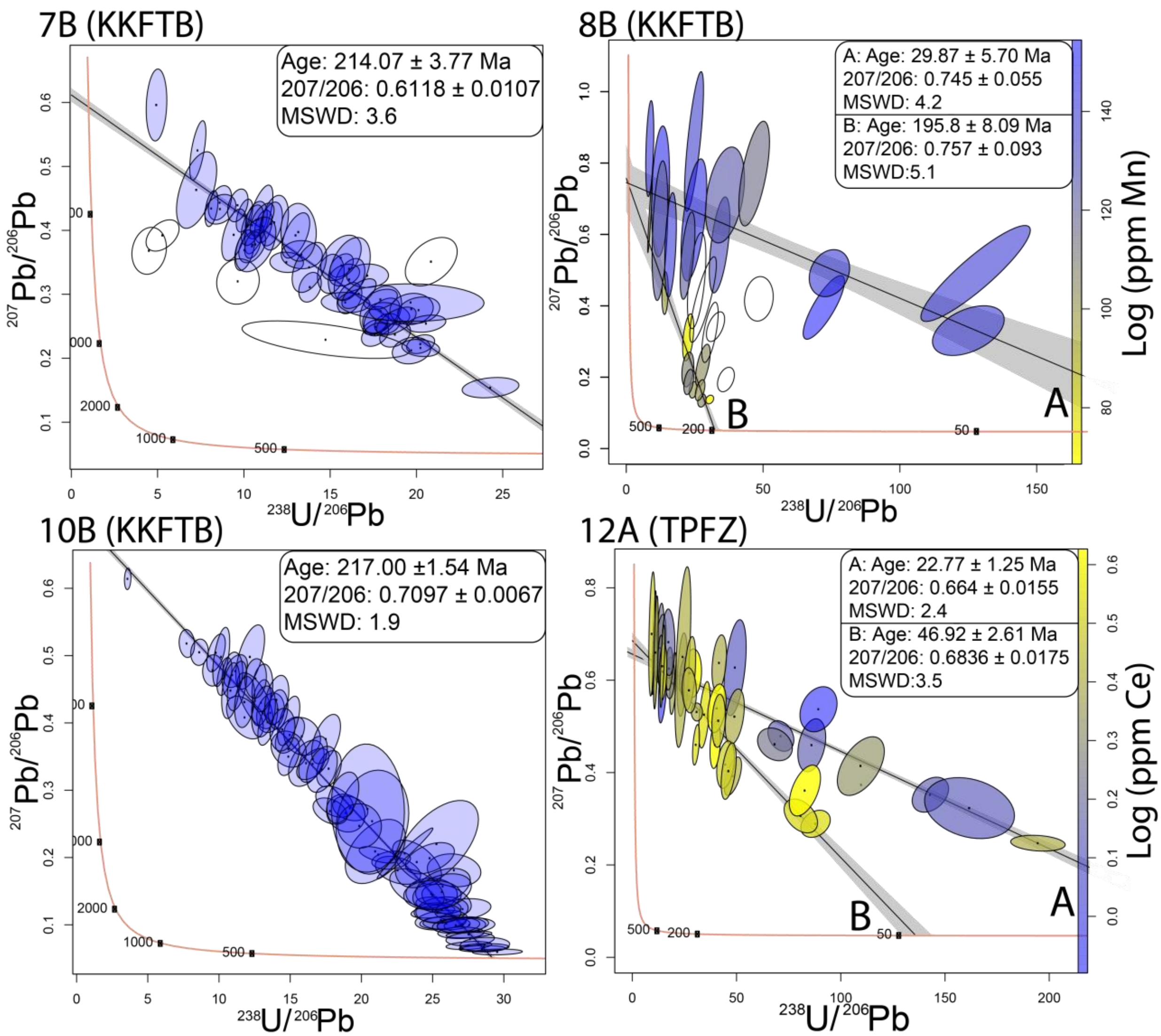

Figure 8. Tera-Wassurburg Concordia plots of successful samples. Samples 7b, 8b, and 10b from the TPFZ, sample 12a from the KKFTB. 8b concentration scale is log(Ce ppm), capped at 0.6 to remove outliers. 12a concentration scale is log(Mn ppm), capped at 2.15 to remove outliers. Each ellipse represents the 2σ uncertainty on the $^{207}Pb/^{206}Pb$ and $^{238}U/^{206}Pb$ ratios for individual laser spots. Uncertainties on the lower intercept ages are at 95% confidence level. Open ellipses show analyses removed due to probable contamination). Plots made using isoplotR (Vermeesch 2018)

4.2.1 KKFTB samples

Sample 7b yields a lower intercept age of 214 ± 4 Ma with an MSWD of 3.6, based on 54 spot analyses. The upper intercept $^{207}Pb/^{206}Pb$ composition determined from the unconstrained regression in Tera-Wasserburg plot is 0.612 ± 0.011. Sample 8b yields a scattered array of data in Tera-Wasserburg space, from which two regression trends can be identified that correlate with the different trace element chemical compositions. More specifically, the two imprecise regressions correlate with different Mn concentrations and define calcite U-Pb dates of 196 ± 8 Ma (MSWD = 5.1) and 29.9 ± 5.7 Ma (MSWD = 4.2), and upper intercept compositions of 0.757 ± 0.093 and 0.745 ± 0.055, respectively. Sample 10b yields a robust lower intercept age of 217 ± 2 Ma, with an MSWD of 1.9.

Elevated Al concentrations were used as a proxy for detrital input in sample 8b, and associated spots were discarded (fig. 6). Additionally, data points were discarded based on significantly anomalous U and Mn values associated with cracks through the calcite samples.

4.2.2 TPFZ samples

Sample 12a from the TPFZ yields a scattered array that likely represents a protracted age range of calcite crystallisation/recrystallization, given the correlation with chemical composition. Using Ce as a chemical denominator, the data can be split into two arrays with lower intercept ages of 46.9 ± 2.6 Ma (MSWD = 3.5) and 22.77 ± 1.25 Ma (MSWD = 3.8), and upper intercept $^{207}Pb/^{206}Pb$ compositions of 0.684 ± 0.018 and 0.663 ± 0.011, respectively.

5 Discussion

5.1 Initial lead compositions

All of the samples dated show significantly lower initial (i.e. common) Pb ratios ($^{207}Pb/^{206}Pb$) than would be expected based on the traditional two part terrestrial evolution model of the earth [*Stacey and Kramers*, 1975]. This indicates that the fluid that the calcite precipitated from contained abundant radiogenic lead, which cannot be sourced from the Ordovician host limestone, as this would not generate particularly radiogenic values in the required timeframe. Instead, radiogenic lead sourced from uraniferous minerals in the surrounding siliciclastic rocks, or those at depth, is required to generate such radiogenic (i.e. low $^{207}Pb/^{206}Pb$) initial compositions [*Roberts*, 2018]. This implies that a significant amount of fluid-rock interaction has undergone prior to vein precipitation, rather than the vein-forming fluids being purely comprised of percolating meteoric water. Additionally, this indicates that common lead corrections utilizing assumed *Stacey and Kramers* [1975] model compositions will be inaccurate, as pointed out by [*Roberts*, 2018], and that a 'free regression' utilising an array of radiogenic to non-radiogenic data is preferred for accurate lower intercept $^{238}U/^{206}Pb$ age determinations.

The analysed samples generally have higher MSWDs than would be expected for a normally distributed single population. These higher MSWDS, however, are generally in line with the expected scatter caused by heterogeneous initial Pb [*Rasbury and Cole*, 2009], as may be expected if fluids are a mixture of local and meteoric sources. A similar observation was made by *Roberts and Walker* [2016]. Additional scatter may also be due to the presence of small inclusions ablated as a result of the large (110 μm) laser spot size used, or minor U or Pb migration along cracks, grain boundaries or cleavage planes. Thermally activated Pb loss is considered unlikely as an explanation for the initial Pb ratios and higher MSWDs, because diffusive mobility of lead is very slow at temperatures below 400°C (Cherniak, 1997).

5.2 Timing of the Khao Kwang Fold and Thrust Belt

Sample 7b was taken from a thrust fault in a fault propagation fold in the KKFTB. This fault was hypothesised to have been active during the late Indosinian Orogeny. The obtained calcite U-Pb date of 214 ± 4 Ma (Fig. 8) confirms the hypothesis and constrains the timing of calcite growth to the Indosinian II deformation phase [roughly ~220 – 190Ma; *Morley et al.*, 2013]. Structural observations suggest that sample 10b was sourced from a bedding-parallel vein that formed in relation to flexural slip and folding (Table 1). This sample (10b) gave the most precise age of the successfully analysed samples (217 ± 2 Ma), with an analytical uncertainty of just 1%. These data demonstrate that calcite U-Pb dating has the potential to date brittle faulting and folding with a high degree of precision using the LA-ICP-QMS method, even at sub-ppm Uranium concentrations.

Sample 8b is of particular interest due to the presence of multiple U-Pb data populations (Fig. 8). This sample was taken from an explosion breccia in close proximity to a strike-slip fault, where field observations indicate that this fault was mostly likely active during the Cenozoic India-Eurasia collision. Two regression lines were calculated through the two U-Pb populations and have been labelled A (~30 Ma) and B (~196 Ma) in figure 8. A possible third age population (few open ellipses, age ~135 Ma, fig. 8) is most likely a mixing age between the two other populations.

Elemental mapping of sample 8b revealed the presence of high Al and elevated U (up to 1500% increase) along cracks (Fig. 6). We interpret this as due to another mineral phase (such as clay) or alteration due to fluid flow along the cracks, and thus associated laser spots were removed. The two U-Pb age populations in this sample, identified above, appear to be spatially distinguishable by Mn zonation (Fig. 6). Chemical zonation within calcite may represent changes in fluid chemistry (and thus potentially different fluid-flow events), or changes in uptake of metals [e.g. *Barker and Cox*, 2011; *Paquette and Reeder*, 1995; *Reeder et al.*, 1990]. Experimental evidence [*Frank et al.*, 1982] demonstrates that Mn can show oscillatory zoning during calcite growth, and these authors suggest that this is related to uptake of Mn^{2+} along the calcite crystal surface that inhibits crystal growth. In fact, Mn zonation is the main source of luminescence for calcite in CL imaging [*Frank et al.*, 1982]. Mn zonation in sample 8b, however, does not conform to oscillatory growth patterns (Fig. 6). Given the shape of the Mn zonation and it association with age populations, we consider it more likely that this zonation reflects changes in fluid chemistry between different precipitation/alteration events. It is therefore envisaged that the calcite initially grew during the Indosinian Orogeny (~196 Ma age population), and that parts were subsequently recrystallised or altered in fluid with a higher Mn concentration, associated with a Cenozoic deformation phase (~30 Ma age population).

The ~196 Ma age population (B) in sample 8b corresponds to the later part of the Indosinian Orogeny stage II [*Morley et al.*, 2013]. The younger ~30 Ma age of Sample 8b corresponds with apatite fission track ages (~39-19 Ma) in the vicinity [*Upton*, 1999], as well as with Ar-Ar and U-Pb dates on Cenozoic structures such as the MPFZ [*Lacassin et al.*, 1997]. Therefore, following the interpretation given for the AFT and Ar-Ar dates, sample 8b may record Cenozoic reactivation that can be linked to the far-field effects of the India-Eurasia collision [*Rhodes et al.*, 2005]

5.3 Timing of the Three Pagodas Fault Zone

The timing of the boudin structures in the outcrop along the Three Pagodas Fault Zone was ambiguous from outcrop relationships alone because they, along with bedding, are rotated by short wavelength (10's m) folds. Since folding is most typically associated with the Indosinian Orogeny, it was highly uncertain whether the boudins were related to Cenozoic strike-slip deformation, or Triassic deformation. U-Pb dating of calcite is likely the only direct method available to resolve this issue with absolute constraints. Successful age determinations were obtained from one of the 'boudin' like zones from a sample (12a), which can be described as a 'floating clast breccia zone', bounded by pressure solution seams. This sample likely formed from repeated hydrofracturing related to activity along the fault zone. The sample appears to contain two age populations: population A at ~23 Ma which correlates with the beginning of a proposed period of dextral motion along the TPFZ at ~23.5 Ma [*Lacassin et al.*, 1997]; and population B at ~47 Ma, which may show earlier activity along the fault, potentially corresponding to the initial sinistral transpressional phase (fig. 8). This ~45 Ma date correlates with activity along the nearby Ranong and Khlong Marui faults at ~48 Ma (Watkinson et al., 2011). Similar zircon U-Pb ages have been found regionally, often associated with rims of ~57 – 51 Ma [*Nantasin et al.*, 2012] and ~45 Ma [*Österle et al.*, 2019].

Populations A and B are from a section of the sample in which multiple veins intersect. These populations can be distinguished by several trace elements including the REE (primarily Ce) (Fig. 7) and Mg zonation. The element Si was monitored to determine the extent of detrital material present along cracks, and several enriched grain boundaries have been avoided during analysis (Fig. 7). Ce/Yb ratios have been used previously to distinguish between different calcite generations [*Maskenskaya et al.*, 2013]. Furthermore, REE distributions have been proposed as a proxy for diagenetic fluid properties, similar to $\delta^{18}O$ [*Bons et al.*, 2012]. Experimental studies suggest that the LREEs, especially Ce (and Eu), are highly mobile in fluids and are commonly used to track fluid sources [*Migdisov et al.*, 2016; Brugger et al., 2016], thus it is inferred that the changes in LREE concentration for this study represent the variable chemistry of different episodes of calcite precipitation. While Ce was identified as a possibly indicator of extrinsic fluid properties (fluid-fluid/rock mixing or different fluid episodes) by *Barker and Cox* [2011], it was also noted that sector zoning in REEs may occur during precipitation. Thus REE zonation on its own may not be enough to conclusively distinguish between different hydrofracturing events.

Sample 12a shows extensive twinning, which is patchy along its length, and has a width > 5 µm, suggesting Type IV high temperature twins (Fig. 6). These twins would most likely have formed with temperatures exceeding 250^{o}C [*Ferrill et al.*, 2004]. Twinning overprints some of the elemental zonation and grain boundaries, and is thus considered to have occurred at the same time or after the latest (population A) generation of calcite growth/alteration. Thus, the twinning implies that the Cenozoic deformation, as young as ~23 Ma, occurred at maximum temperatures in excess of 250^{O}C. This is consistent with regional Ar-Ar biotite geochronology (~24 Ma) in the vicinity of the sample location, which implies cooling below ~300^{o}C [*Lacassin et al.*, 1997]. The similarities between dates and temperatures for calcite and biotite growth, implies twin formation occurred during or soon after the ~23 Ma episode of calcite precipitation.

Overall, our data suggest a protracted crystallisation or fluid-based resetting of calcite from at least 47 to 23 Ma. The correlation between age and chemistry, and the existence of the high temperature twins, suggests that the different ages do not simply represent U-mobility due to fluid-based alteration, but reflect different fluid infiltration events with different fluid chemistries, and that these occurred under high temperature conditions. A key tenet of this dating method is to determine whether fluid-flow can outlast brittle deformation, which would limit the utility of the method for dating the latter. It is always difficult to rule this out, but in this case we argue that the different ages reflect fluid infiltration during successive hydrofracturing events, and thus provide constraints on deformation as well as fluid-flow.

6 Conclusions

(1) U-Pb dating and elemental mapping of calcite precipitated in tectonic veins can be used to constrain the timing of tectonic events. There are, however, limitations, related to low U concentrations and potentially complex data.As shown in this study, cathodoluminescence and trace element (laser) imaging can greatly enhance our understanding of complex U-Pb calcite data.

(2) Dating of calcite hydrofracturing and brecciation can be useful in constraining different episodes of tectonic movement, but detailed *in-situ* chemical and textural analysis are required to link calcite dates to specific fluid-flow and deformation events.

(3) Calcite can host microscale differences in age as well as chemistry, which should be taken into account during analysis. Redox-sensitive (and fluid mobile) elements such as Mn and REEs, may be a useful proxy for investigating these differences.

(4) The KKFTB deformed during the mid-Late Triassic. In more detail, U-Pb dating of calcite has identified specific fracturing events occurring at ~216 Ma and 209 Ma associated with individual structures during Stage II of the Indosinian Orogeny. The precise dating of calcite associated with flexural slip (bedding plane slip) of a fold structure, indicates such calcite veins can remain a closed isotopic system, and might be particularly useful for dating structural events.

(5) Calcite data from this study, integrated with previous dating results, suggest a two-stage brittle deformation history for the TPFZ at ~52-45 Ma and at ~23-18 Ma.

(6) Previously it was uncertain whether the unusual boundinaged, pressure solution structures within the Ordovician Limestones were related to motion on the Cenozoic Three Pagodas Fault Zone, or the Triassic Indosinian Orogeny. Dating of the calcite veins has established that these structures are of Cenozoic age.

Acknowledgments

This study was supported by an Australian Research Council Discovery grant (DP150101730) and a University of Adelaide student support grant. Sarah Gilbert is thanked for assistance with the LA-ICP-MS facility. Gilby Jepson and Angus Nixon are also thanked for their help.

Supplementary data for this paper can be accessed at https://adelaide.figshare.com/articles/Calcite_Thailand_Supp_data_1_xlsx/11565732

References

Al-Aasm, I. (2003), Origin and characterization of hydrothermal dolomite in the Western Canada Sedimentary Basin, *Journal of Geochemical Exploration*, *78-79*, 9-15.

Arboit, F., K. Amrouch, A. S. Collins, R. King, and C. K. Morley (2015), Determination of the tectonic evolution from fractures, faults, and calcite twins on the southwestern margin of the Indochina Block, *Tectonics*, *34*(8), 1576-1599.

Arboit, F., A. S. Collins, C. K. Morley, R. King, and K. Amrouch (2016), Detrital zircon analysis of the southwest Indochina terrane, central Thailand: Unravelling the Indosinian orogeny, *Geological Society of America Bulletin*, *128*(5-6), 1024-1043.

Arboit, F., K. Amrouch, C. K. Morley, A. S. Collins, and R. King (2017), Palaeostress magnitudes in the Khao Khwang fold-thrust belt, new insights into the tectonic evolution of the Indosinian orogeny in central Thailand, *Tectonophysics*, *710-711*, 266-276.

Barber, A. J., M. F. Ridd, and M. J. Crow (2011), The origin, movement and assembly of the pre-Tertiary tectonic units of Thailand

The Geology of Thailand, edited by M. F. Ridd, A. J. Barber and M. J. Crow, p. 0, Geological Society of London.

Barker, S. L. L., and S. F. Cox (2011), Oscillatory zoning and trace element incorporation in hydrothermal minerals: insights from calcite growth experiments, *Geofluids*, *11*(1), 48-56.

Barr, S. M., and A. S. Macdonald (1987), Nan River suture zone, northern Thailand, *Geology*, *15*(10).

Bons, P. D., M. A. Elburg, and E. Gomez-Rivas (2012), A review of the formation of tectonic veins and their microstructures, *Journal of Structural Geology*, *43*, 33-62.

Davies, G. R., and L. B. Smith (2006), Structurally controlled hydrothermal dolomite reservoir facies: An overview, *AAPG Bulletin*, *90*(11), 1641-1690.

Dew, R. E. C., R. King, A. S. Collins, C. K. Morley, F. Arboit, and S. Glorie (2018a), Stratigraphy of deformed Permian carbonate reefs in Saraburi Province, Thailand, *Journal of the Geological Society*, *175*(1), 163-175.

Dew, R. E. C., et al. (2018b), Probing into Thailand's basement: New insights from U–Pb geochronology, Sr, Sm–Nd, Pb and Lu–Hf isotopic systems from granitoids, *Lithos*, *320-321*, 332-354.

Eichhubl, P., and J. R. Boles (2000a), Rates of Fluid Floe in Fault Systems - Evidence for Episodic Rapid Fluid Flow in the Miocene Monterey Formation, Coastal California, *American Journal of Science*, *300*, 571-600.

Eichhubl, P., and J. R. Boles (2000b), Focused fluid flow along faults in the Monterey Formation, coastal California, *GSA Bulletin*, *112*(11), 1667-1679.

Farkaš, J., J. Frýda, and C. Holmden (2016), Calcium isotope constraints on the marine carbon cycle and CaCO 3 deposition during the late Silurian (Ludfordian) positive δ 13 C excursion, *Earth and Planetary Science Letters*, *451*, 31-40.

Ferrill, D. A., A. P. Morris, M. A. Evans, M. Burkhard, R. H. Groshong, and C. M. Onasch (2004), Calcite twin morphology: a low-temperature deformation geothermometer, *Journal of Structural Geology*, *26*(8), 1521-1529.

Frank, J. R., A. B. Carpenter, and T. W. Oglesby (1982), Cathodoluminescence and Composition of Calcite Cement in the Taum Sauk Limestone (Upper Cambrian), Southeast Missouri, *1982*, *52*(2), 0631-0638.

Gardiner, N. J., L. J. Robb, C. K. Morley, M. P. Searle, P. A. Cawood, M. J. Whitehouse, C. L. Kirkland, N. M. W. Roberts, and T. A. Myint (2016), The tectonic and metallogenic framework of Myanmar: A Tethyan mineral system, *Ore Geology Reviews*, *79*, 26-45.

Hansberry, R. L., R. King, A. S. Collins, and C. K. Morley (2014), Complex structure of an upper-level shale detachment zone: Khao Khwang fold and thrust belt, Central Thailand, *Journal of Structural Geology*, *67*, 140-153.

Hansberry, R. L., H. Zwingmann, S. Loehr, A. S. Collins, R. C. King, C. K. Morley, and R. N. Drysdale (2017), Constraining the timing of shale detachment faulting: A geochemical approach, *Lithosphere*, *9*(3), 431-440.

Hansberry, R. L., A. S. Collins, R. C. King, C. K. Morley, A. P. Giże, J. Warren, S. C. Löhr, and P. A. Hall (2015), Syn-deformation temperature and fossil fluid pathways along an exhumed detachment zone, khao khwang fold-thrust belt, Thailand, *Tectonophysics*, *655*, 73-87.

Hansen, B. T., and K. Wemmer (2011), Age and evolution of the basement rocks in Thailand, in *The Geology of Thailand*, edited by M. F. Ridd, A. J. Barber and M. J. Crow, p. 0, Geological Society of London.

Huchon, P., X. Le Pichon, and C. Rangin (1994), Indochina Peninsula and the Collision of India and Eurasia, *Geology*, *22*, 27-30.

Lacassin, R., H. Maluski, P. H. Leloup, P. Tapponnier, C. Hinthong, K. Siribhakdi, S. Chuaviroj, and A. Charoenravat (1997), Tertiary diachronic extrusion and deformation of western Indochina: Structural and40Ar/39Ar evidence from NW Thailand, *Journal of Geophysical Research: Solid Earth*, *102*(B5), 10013-10037.

Leloup, P. H., N. Arnaud, J. R. Lacassin, J. R. Kienast, T. M. Harrison, T. T. Phan Trong, A. Replumaz, and P. Tapponier (2001), New Constraints on hte Structure, thermichronology, and timing of the Ailao Shan-REd River Shear Zone, SE Asia, *Journal of Geophysical Research*, *106*(B4), 6683-6732.

Li, Q., R. R. Parrish, M. S. A. Horstwood, and J. M. McArthur (2014), U–Pb dating of cements in Mesozoic ammonites, *Chemical Geology*, *376*, 76-83.

Maskenskaya, O. M., H. Drake, and M. E. Åström (2013), Geochemistry of Calcite Veins: Records of Fluid Mixing and Fluid-Rock Interaction, *Procedia Earth and Planetary Science*, *7*, 566-569.

Migdisov, A., A. E. Williams-Jones, J. Brugger, and F. A. Caporuscio (2016), Hydrothermal transport, deposition, and fractionation of the REE: Experimental data and thermodynamic calculations, *Chemical Geology*, *439*, 13-42.

Morley, C. K. (2002), A tectonic model for the Tertiary evolution of strike–slip faults and rift basins in SE Asia, *Tectonophysics*, *347*(4), 189-215.

Morley, C. K. (2009), Geometry and evolution of low-angle normal faults (LANF) within a Cenozoic high-angle rift system, Thailand: Implications for sedimentology and the mechanisms of LANF development, *Tectonics*, *28*(5), n/a-n/a.

Morley, C. K. (2018), Understanding Sibumasu in the context of ribbon continents, *Gondwana Research*, *64*, 184-215.

Morley, C. K., and A. Racey (2011), Tertiary stratigraphy
The Geology of Thailand, edited by M. F. Ridd, A. J. Barber and M. J. Crow, p. 0, Geological Society of London.

Morley, C. K., and A. Racey (2011), Tertiary stratigraphy, in *The Geology of Thailand*, edited by M. F. Ridd, A. J. Barber and M. J. Crow, p. 0, Geological Society of London.

Morley, C. K., P. Charusiri, and I. M. Watkinson (2011), Structural geology of Thailand during the Cenozoic

The Geology of Thailand, edited by M. F. Ridd, A. J. Barber and M. J. Crow, p. 0, Geological Society of London.

Morley, C. K., M. Smith, A. Carter, P. Charusiri, and S. Chantraprasert (2007), Evolution of deformation styles at a major restraining bend, constraints from cooling histories, Mae Ping fault zone, western Thailand, *Geological Society, London, Special Publications*, *290*(1), 325-349.

Morley, C. K., P. Ampaiwan, S. Thanudamrong, N. Kuenphan, and J. Warren (2013), Development of the Khao Khwang Fold and Thrust Belt: Implications for the geodynamic setting of Thailand and Cambodia during the Indosinian Orogeny, *Journal of Asian Earth Sciences*, *62*, 705-719.

Nachtergaele, S., S. Glorie, C. K. Morley, P. Charusiri, P. Kanjanapayont, P. Vermeesch, A. Carter, G. Van Ranst, and J. De Grave (2019), Cenozoic tectonic evolution of southeastern Thailand derived from low-temperature thermochronology, *Journal of the Geological Society*.

Nantasin, P., C. Hauzenberger, X. Liu, K. Krenn, Y. Dong, M. Thöni, and P. Wathanakul (2012), Occurrence of the high grade Thabsila metamorphic complex within the low grade Three Pagodas shear zone, Kanchanaburi Province, western Thailand: Petrology and geochronology, *Journal of Asian Earth Sciences*, *60*, 68-87.

Nazrul, M. (2015), Fluid Evolution Through Different Deformation Stages: A Carbonate Outcrop-Based Study in the Western Highland of Thailand, 39 pp, Chulalongkorn University, Thailand.

Nuriel, P., R. Weinberger, A. R. C. Kylander-Clark, B. R. Hacker, and J. P. Craddock (2017), The onset of the Dead Sea transform based on calcite age-strain analyses, *Geology*, *45*(7), 587-590.

Österle, J. E., U. Klötzli, D. F. Stockli, M. Palzer-Khomenko, and P. Kanjanapayont (2019), New age constraints on the Lan Sang gneiss complex, Thailand, and the timing of activity of the Mae Ping shear zone from in-situ and depth-profile zircon and monazite U-Th-Pb geochronology, *Journal of Asian Earth Sciences*, *181*.

Palin, R. M., M. P. Searle, C. K. Morley, P. Charusiri, M. S. A. Horstwood, and N. M. W. Roberts (2013), Timing of metamorphism of the Lansang gneiss and implications for left-lateral motion along the Mae Ping (Wang Chao) strike-slip fault, Thailand, *Journal of Asian Earth Sciences*, *76*, 120-136.

Paquette, J., and R. J. Reeder (1995), Relationship between surface structure, growth mechanism, and trace element incorporation in calcite, *Geochimica et Cosmochimica Acta*, *59*(4), 735-749.

Paton, C., J. Hellstrom, B. Paul, J. Woodhead, and J. Hergt (2011), Iolite: Freeware for the visualisation and processing of mass spectrometric data, *Journal of Analytical Atomic Spectrometry*, *26*(12).

Petrus, J. A., D. M. Chew, M. I. Leybourne, and B. S. Kamber (2017), A new approach to laser-ablation inductively-coupled-plasma mass-spectrometry (LA-ICP-MS) using the flexible map interrogation tool 'Monocle', *Chemical Geology*, *463*, 76-93.

Rasbury, E. T., and J. M. Cole (2009), Directly dating geologic events: U-Pb dating of carbonates, *Reviews of Geophysics*, *47*(3).

Reeder, R. J., R. O. Fagioli, and W. J. Meyers (1990), Oscillatory Zoning of Mn in Solution-grown Calcite Crystals, *Earth-Science Reviews*, *29*, 39-46.

Rhodes, B. P., P. Charusiri, S. Kosuwan, and A. Lamjuan (2005), Tertiary Evolution of the Three Pagodas Fault, Western Thailand, in *Proceedings of the International Conference on Geology, Geotechnology and Mineral Resources of Indochina*, edited, pp. 498-505, Khon Kaen, Thialand.
Ridd, M. F., A. J. Barber, and M. J. Crow (2011), Introduction to the geology of Thailand
The Geology of Thailand, edited by M. F. Ridd, A. J. Barber and M. J. Crow, p. 0, Geological Society of London.
Roberts, N. M. W. (2018), Progress in Crustal deformation and fluid-flow using U-Pb carbonate geochronology, in *15th International Conference on Gondwana to Asia IAGR*, edited, pp. 69-70, Xian, China.
Roberts, N. M. W., and R. J. Walker (2016), U-Pb geochronology of calcite-mineralized faults: Absolute timing of rift-related fault events on the northeast Atlantic margin, *Geology*, *44*(7), 531-534.
Roberts, N. M. W., E. T. Rasbury, R. R. Parrish, C. J. Smith, M. S. A. Horstwood, and D. J. Condon (2017), A calcite reference material for LA-ICP-MS U-Pb geochronology, *Geochemistry, Geophysics, Geosystems*, *18*(7), 2807-2814.
Searle, M. P., and C. K. Morley (2011), Tectonic and thermal evolution of Thailand in the regional context of SE Asia
The Geology of Thailand, edited by M. F. Ridd, A. J. Barber and M. J. Crow, p. 0, Geological Society of London.
Sibson, R. H. (1996), Structural permeability of fluid-driven fault-fracture meshes, *Journal of Structural Geology*, *18*(8), 1031-1042.
Sone, M., and I. Metcalfe (2008), Parallel Tethyan sutures in mainland Southeast Asia: New insights for Palaeo-Tethys closure and implications for the Indosinian orogeny, *Comptes Rendus Geoscience*, *340*(2-3), 166-179.
Stacey, J. S., and J. D. Kramers (1975), Approximation of terrestrial lead isotope evolution by a two-stage model, *Earth and Planetary Science Letters*, *26*(2), 207-221.
Ueno, K., and T. Charoentitirat (2011), Carboniferous and Permian, in *The Geology of Thailand*, edited by M. F. Ridd, A. J. Barber and M. J. Crow, p. 0, Geological Society of London.
Ueno, K., A. Miyahigashi, and T. Charoentitirat (2010), The Lopingian (Late Permian) of mid-oceanic carbonates in the Eastern Palaeotethys: stratigraphical outline and foraminiferal faunal succession, *Geological Journal*, *45*(2-3), 285-307.
Upton, D. R. (1999), A Regional Fission Track Study of Thailand: Implications for Thernal Histroy and Denudation, Birkbeck (University of London).
Vermeesch, P. (2018), IsoplotR: A free and open toolbox for geochronology, *Geoscience Frontiers*, *9*(5), 1479-1493.
Warren, J., C. K. Morley, T. Charoentitirat, I. Cartwright, P. Ampaiwan, P. Khositchaisri, M. Mirzaloo, and J. Yingyuen (2014), Structural and fluid evolution of Saraburi Group sedimentary carbonates, central Thailand: A tectonically driven fluid system, *Marine and Petroleum Geology*, *55*, 100-121.
Watkinson, I., C. Elders, G. Batt, F. Jourdan, R. Hall, and N. J. McNaughton (2011), The timing of strike-slip shear along the Ranong and Khlong Marui faults, Thailand, *Journal of Geophysical Research: Solid Earth*, *116*(B9).

Table 1:

Sample number	Coordinates	Description (see figure x for pictures)	Vein Style
Khao Kwang Fold and Thrust belt (KKFTB)			
7b	14 42.266'N, 100 53.122'E	Sampled from an out of sequence thrust zone in a fault-propagation-fold. Deformation is hypothesised to be Indosinian in age.	Folded vein that runs across the bedding. Calcite crystals are 'blocky' and are consistent with fracture infill
8b	14 42.783N, 100.52.250'E	Sampled from an over-pressured \`explosion\` brecciated limestone. Thought to be Cenozoic in age.	The sample is made up of 2 well-developed calcite crystals.
10b	14 36.554N, 101 23.478E	Sampled from a folded vein, associated with flexural slip. Hypothesised to be Indosinian stage II.	Blocky crystals, no obvious growth direction, Calcite shows textural variation within veins.
Three Pagodas Fault zone (TPFZ)			
12a	14 14.011N, 99 14.303E	Sampled in a road cutting on highway 3199 (near Chong Sadao). Sample from a fault breccia formed from hydrofracturing. Hypothesised to be Cenozoic.	Calcite crystal shape not consistent with 'normal' fracture infill. This is probably due to being related to pressure solution during periods of hydrofracturing.

Table 1. Sample locations and descriptions